



Simplified Formulations for Estimating the Main Frequencies of Ancient Masonry Churches

Saulo Lopez^{1*}, Michele D'Amato^{1*}, Luis Ramos², Michelangelo Laterza^{1†} and Paulo B. Lourenço²

¹ DICEM, Department of European and Mediterranean Cultures (Architecture, Environment and Cultural Heritage), University of Basilicata, Matera, Italy, ² Department of Civil Engineering, ISISE, University of Minho, Guimarães, Portugal

OPEN ACCESS

Edited by:

Solomon Tesfamariam,
University of British Columbia, Canada

Reviewed by:

Michele Betti,
Università degli Studi di Firenze, Italy
Antonio Formisano,
University of Naples Federico II, Italy

*Correspondence:

Michele D'Amato
michele.damato@unibas.it
Saulo Lopez
saulo.lopezm@pucp.pe

[†] Michelangelo Laterza was the coordinator of the ELARCH mobility network. He had a true passion for research and conservation of historic buildings, and left us unexpectedly in August 2018

Specialty section:

This article was submitted to Earthquake Engineering, a section of the journal *Frontiers in Built Environment*

Received: 13 December 2018

Accepted: 07 February 2019

Published: 06 March 2019

Citation:

Lopez S, D'Amato M, Ramos L, Laterza M and Lourenço PB (2019) Simplified Formulations for Estimating the Main Frequencies of Ancient Masonry Churches. *Front. Built Environ.* 5:18. doi: 10.3389/fbuil.2019.00018

This paper proposes simplified formulations for estimating the main frequencies of ancient masonry churches. The formulations are derived starting from the results of numerical analyses with finite elements models, whose geometric parameters are assigned in accordance with specific relationships established on a set of 50 existing churches. The so-obtained formulations are also compared with the results of a series of experimental dynamic identification tests chosen from literature. Finally, starting from these experimental results, through numerical regressions, formulas for predicting the main frequencies of ancient masonry churches are proposed, too.

Keywords: churches, cultural heritage, masonry, numerical models, vibration frequency

INTRODUCTION

The knowledge of the dynamic properties of a structure in the linear range is fundamental, because they influence the response evolution within the non-linear field. If the seismic lateral excitation is concerned, modal response characteristics, such as shape and frequency of vibration modes and damping ratios, are important not only for predicting the seismic performance (Ramos et al., 2013; D'Amato et al., 2017; Laterza et al., 2017), but also for diagnosing the current condition of a structure (Ramos et al., 2010; Ranieri and Fabbrocino, 2011). In fact, modal dynamic properties allow evaluating the effective connection among the parts, as well as allow obtaining progressive or sudden damage occurring while the structure is in service or after an exceptional action such as an earthquake. Moreover, from a computational point of view, the fundamental period is very important in order to apply analytical methods having a different level of refinement for estimating the response of masonry structures/elements. A recent discussion and application of such methods, with a particular reference to ancient masonry structures, may be found for instance, among the others, in Lagomarsino and Resemini (2009); Lourenço et al. (2013); Caprili et al. (2017); Formisano and Marzo (2017); D'Amato et al. (2018); Fuentes et al. (2019). More in general, a discussion of the significance of *in-situ* tests on ancient masonry structures may be found in Krstevska et al. (2010); Formisano et al. (2018), and in Luchin et al. (2018).

From a conceptual point of view the dynamic behavior of a structure may be studied using two different approaches: *an analytical approach*, in which starting from geometry, damping, distribution of mass and stiffness it is possible to calculate in a closed form the modal characteristics of the system; and *an experimental approach*, in which starting from the experimental structural response under a certain excitation it is possible to estimate the dynamic properties of a structure, such as frequencies, vibration modes, and damping by applying dynamic identification techniques. The analytical approach, known as *direct problem*, requires the definition of a numerical model.

The experimental approach, also known as indirect problem since it starts from measurements data for estimating system properties, requires the availability of an equipment for monitoring structures. The first applications of dynamic structural identification were carried out in the 1970s for performing damage identification of aerospace structures and offshore platforms. Also, it should be mentioned the pioneer activity carried out by Ellis and BRE (1998) in order to evaluate the integrity of 534 stone pinnacles on the Westminster Palace. Nowadays, this technique is widespread also for civil engineering purposes, aiming at the evaluation of the structural behavior along the time (Douglas and Reid, 1982) also in the case of historical constructions (among the others Casarin and Modena, 2007; Ranieri et al., 2013; De Luca et al., 2014).

Starting from these premises, the present paper focuses on the estimation, through an analytical approach, of the main natural frequencies of ancient masonry churches, which are useful for seismic assessment purposes. First, equations indicated in national codes to estimate the main frequencies of a structure are examined and compared. Then, a series of parametric numerical simulations are carried out in order to propose new equations for estimating the main vibration modes frequencies of ancient masonry churches. The equations are derived by considering two different churches typologies, having one or three naves. For each typology, four possible different configurations are defined as function of roof and bell tower configuration. The parametric analyses are performed by varying the defined fundamental geometric parameters of the considered numerical models. Based on the obtained results, exponential regressions with multiple variables are proposed for the transversal and longitudinal main frequencies of vibration modes, taking into account geometric parameters and Young's modulus. The obtained correlations are also compared with the results of dynamic identifications tests performed in several case studies, whose results are available in literature. Finally, a correction of the proposed equations numerically derived for the first main frequency is discussed on the basis of the comparison with the experimental results.

The proposed formulas are particularly useful since they are proposed for ancient churches structural typologies, while the existing national code formulations are referred, on the contrary, to generic buildings. They also represent a practical tool for revealing potential hidden damages or for identifying the actual connections among the parts, since their results may be compared with the ones obtained through on site dynamic identification tests.

ESTIMATION OF MAIN MODAL FREQUENCY WITH EXISTING NATIONAL CODES EQUATIONS

Generally, national codes provide a simplified equation for estimating the main frequency of a structure. These formulas are useful for instance for static seismic analyses, in which the distribution of static lateral forces is determined in a simplified way, avoiding to perform a modal linear analysis.

In this work three different formulas are analyzed and compared. In particular, they are taken into account formulas indicated in the American (ASCE 07-16, 2017), the Italian (NTC-2008, 2008), and the Spanish (NCSE-2002, 2002). It should be noted that these are established through empirical correlations primarily depending on the structure building height, reflecting the principle that, if mass and stiffness are kept constant, the higher the height the lower the frequency of the first vibration mode. Moreover, the considered formulations are referred to a general masonry building typology, and not specifically to the ancient churches typology (Goel and Chopra, 1997).

ASCE 07-16 (2017) provides a general expression for calculating the fundamental frequency of a structure. For masonry typology, the following equation is given:

$$f(H) = \frac{1}{0.0488H^{3/4}} \text{ (H in meters)} \quad (1)$$

where f is the natural frequency, H is the structural height of the roof above from the base, not including any parapet or penthouse.

The Italian (NTC-2008, 2008) recommends the following equation to estimate the fundamental frequency of a masonry structure, substantially similar to the (ASCE 07-16, 2017) one:

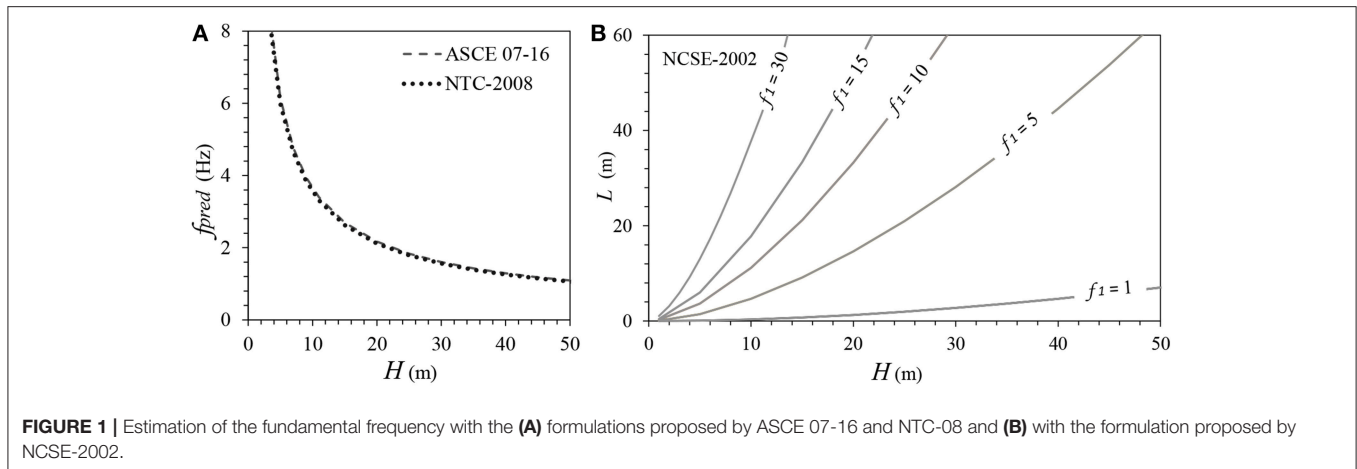
$$f(H) = \frac{1}{0.05H^{3/4}} \text{ (H in meters)} \quad (2)$$

specifying that the equation is used for buildings lower than 40 meters having a uniform mass distributed along the height. It is worthy of note that in the recent updated Italian Design code (NTC-2018, 2018) it is proposed the relationship $f = \frac{1}{(2\sqrt{d})}$, where d is the lateral elastic displacement of the highest point of the structure under the seismic action. This expression presumes that d is known through, at least, a seismic static equivalent analysis, allowing of differentiating the oscillation frequency along the two principal directions. Although it is more complete, in this study it is considered only the Equation (2) since, similarly to the other ones considered, the formula refers directly to geometric properties of the investigated structure.

The Spanish Design Code (NCSE-2002, 2002) suggests a more complete formula, capable of estimating the fundamental frequency in the two principal directions, and also useful for estimating the second and the third natural frequency in the same direction of the first one. The proposed formula takes into account the plan dimension L along the direction of oscillation, as well as the structure height H :

$$f_1 = \frac{\sqrt{L}}{0.06H\sqrt{\frac{H}{2L+H}}}, f_2 = 3f_1, f_3 = 5f_1 \quad (3)$$

For completeness, **Figure 1** graphically illustrates the formulas here considered. In particular, **Figure 1A** depicts the predicted frequencies (f_{pred}) obtained with the (ASCE 07-16, 2017) and (NTC-2008, 2008) formulas. Whereas, **Figure 1B** shows some iso-frequency curves obtained by varying H and L in according to the (NCSE-2002, 2002) equation.



It should be remarked that the previous equations may be applied with particular regard to masonry buildings. They are not specific for ancient masonry churches that should require adequate formulas due to their particular structural typology. A similar approach, for instance, may be found in the recent studied of Shakya et al. (2016); Bartoli et al. (2017); Diaferio et al. (2018); and Sarhosis et al. (2018) where appropriate empirical and semiempirical formulations for predicting the main frequency of slender masonry towers have been proposed.

SIMPLIFIED FORMULATIONS FOR ESTIMATING ANCIENT MASONRY CHURCHES MODAL FREQUENCIES

In order to propose a simplified formulation for estimating the modal frequencies of ancient masonry churches, a set of 50 existing Portuguese case studies having Romanesque, Manueline (Portuguese late Gothic) and Baroque styles are taken into consideration. The location and the architectural style of the each considered church may be found in the Annex. While, **Figure 2A** shows the geographical location of the 50 sampled churches with the corresponding identification number. As it is possible to note, most of churches are located in the northwest, due to the fact that this area was in the past the most influential religious place of the Country. Additionally, in this area it is also possible to find the great nucleus of national Romanesque architecture. Commonly, the masonry encountered consists of local granite blocks due to its abundance, with very thin mortar joints. The texture of the masonry is always really regular and no significant damage is present for each church of the chosen data set.

The chosen churches are identified by typology, considering the plan and spatial composition, the main structural elements and the range of structural measures. They have one or three naves with a Latin cross plan, where the central nave is taller than the lateral ones. Commonly, they have a bell tower adjacent to the main building and, only in some cases, such structures present two towers. The roof system usually consists of masonry vaults or wooden roofs connected by timber beams embedded in the longitudinal walls. In both the cases, roof tiles are placed on these

elements. **Figure 2B** summarizes the classification for single or three naves typology, considering for each of them four sub-cases, as follows: case *Simple* (S) associated to churches having nave(s), a main chapel and timber roof; case *Bell Tower* (T) corresponding to churches with nave(s), main chapel, timber roof and bell tower; case *Vault* (V) for churches with nave(s), main chapel, and vault; and case *Vault and Bell Tower* (VT) for churches with nave(s), main chapel, vault and bell tower. Therefore, by considering the combinations of these four major elements found within the considered database 8 reference typologies, in total, have been individuated.

After classified the considered 50 existing churches in according to the 8 considered reference typologies, the following relationships have been derived through linear regressions between the main geometrical properties, namely, width, length, and height:

- *Single Nave Typology*

$$\left\{ \begin{array}{l} LNV = 2.53 \cdot WNV - 1.61 \quad (R^2 = 0.70) \\ LMAX = 1.33 \cdot LNV + 2.51 \quad (R^2 = 0.96) \\ WMC = 0.62 \cdot WNV + 0.83 \quad (R^2 = 0.74) \\ LNV = 1.49 \cdot HNV + 2.84 \quad (R^2 = 0.71) \\ HNV = 9.90 \cdot Thickness + 2.04 \quad (R^2 = 0.51) \\ HNVmin \text{ not applicable} \\ WBT = 0.28 \cdot WNV + 0.80 \quad (R^2 = 0.61) \\ HBT = 1.7 \cdot HNV \quad (R^2 \text{ not calculable}) \end{array} \right. \quad (4)$$

- *Three Naves Typology*

$$\left\{ \begin{array}{l} LNV = 2.02 \cdot WNV - 1.64 \quad (R^2 = 0.61) \\ LMAX = 1.45 \cdot LNV - 4.95 \quad (R^2 = 0.89) \\ WMC = 0.85 \cdot WNV - 6.09 \quad (R^2 = 0.74) \\ LNV = 1.37 \cdot HNV + 16.37 \quad (R^2 = 0.32) \\ HNV = 9.49 \cdot Thickness + 3.00 \quad (R^2 = 0.57) \\ HNVmin = 0.72 \cdot HN - 0.83 \quad (R^2 = 0.69) \\ WBT = 0.60 \cdot WNV + 4.58 \quad (R^2 = 0.75) \\ HBT = 1.4 \cdot HNV \quad (R^2 \text{ not calculable}) \end{array} \right. \quad (5)$$

Where the considered geometric parameters are (Figures 3A,B): *LMAX*: maximum plan length; *LNV*: length of the nave(s); *WNV*: width of the nave(s); *WBT*: width of the bell tower(s); *WMC*: width of main chapel, *HBT*: height of the bell tower,

HNV_{min}: height of the lateral naves; *HNV*: height of the main nave. For completeness, for each geometrical relationship found among it is reported also the resulting coefficient of correlation (R^2).

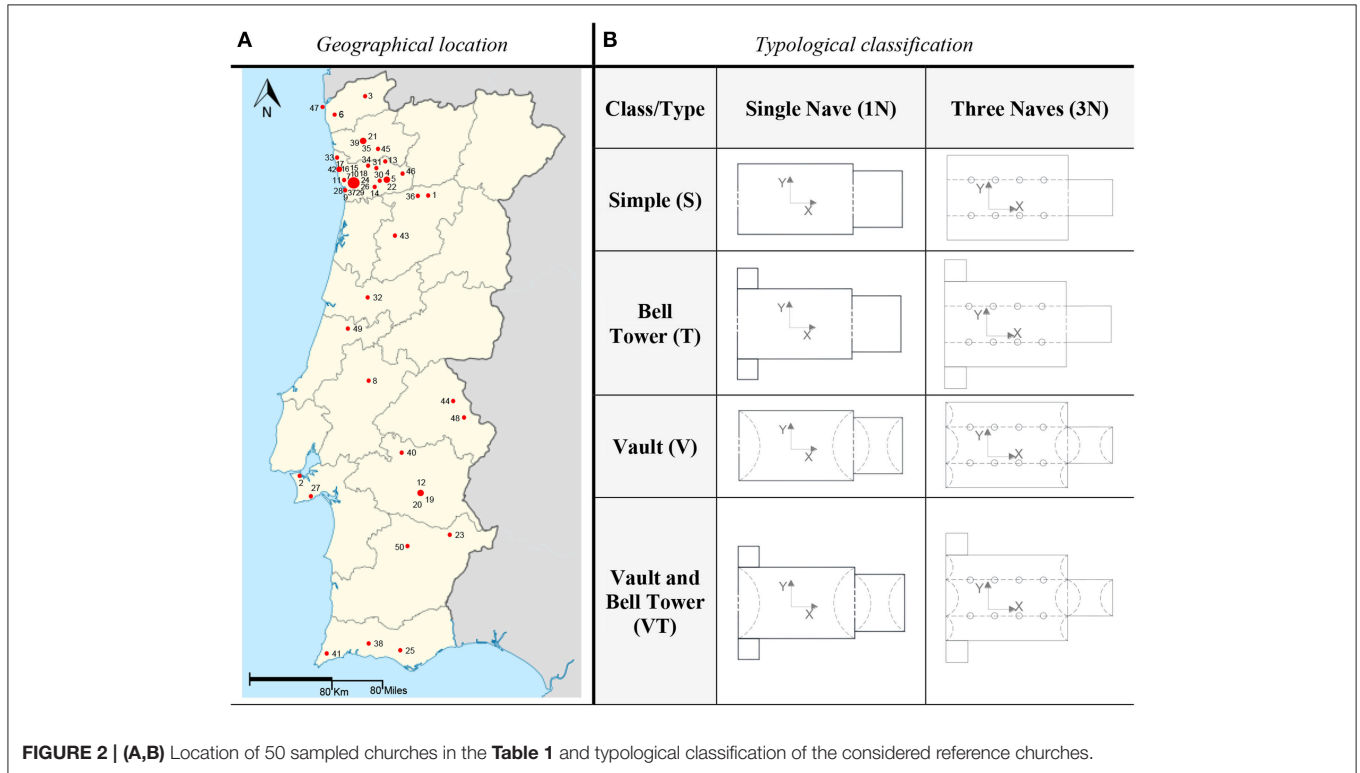


FIGURE 2 | (A,B) Location of 50 sampled churches in the Table 1 and typological classification of the considered reference churches.

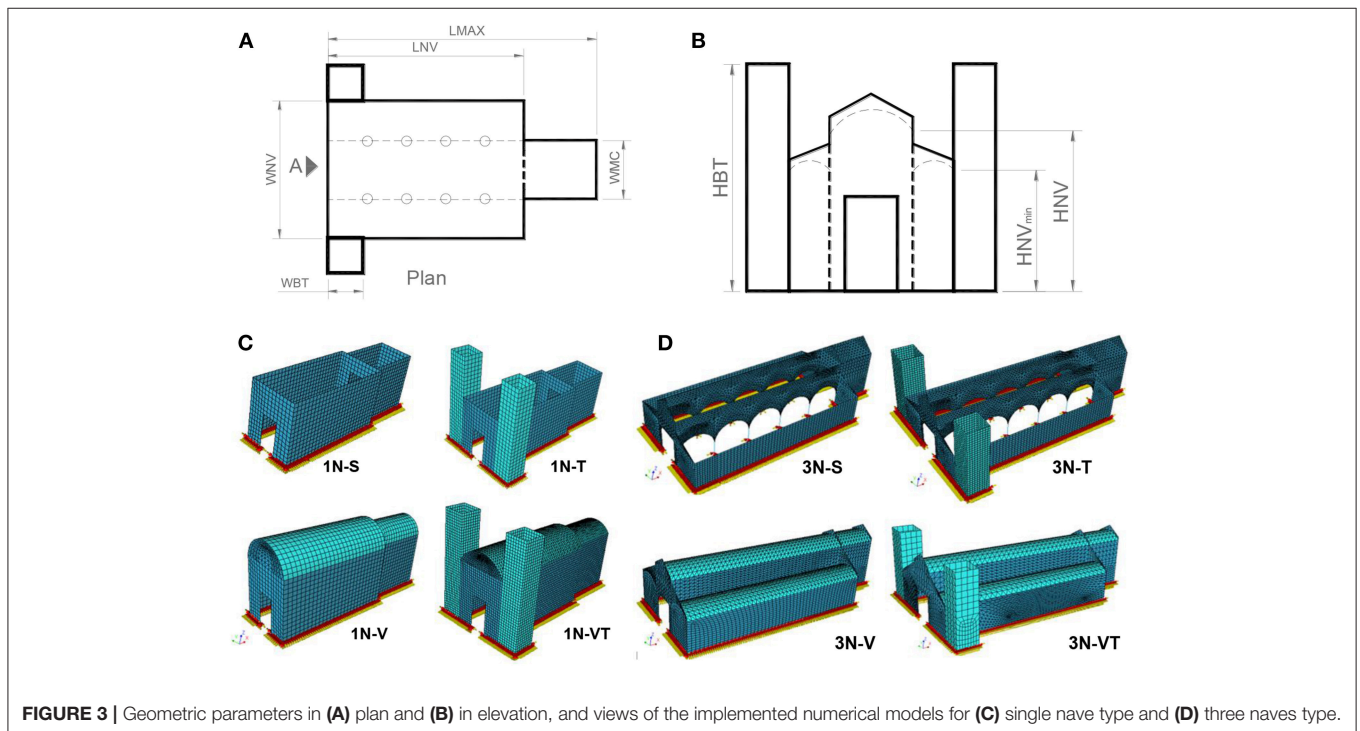


FIGURE 3 | Geometric parameters in (A) plan and (B) in elevation, and views of the implemented numerical models for (C) single nave type and (D) three naves type.

Once the relationships among the main churches geometrical properties have been derived, a series of numerical simulations are carried out in order to numerically predict the natural frequencies of these church models. The simulations are performed by referring to the eight identified reference typologies, whose geometric parameters are assigned considering the relationships reported in the Equation (4) and in the Equation (5). The numerical models are implemented within iDiana 10.1 (TNO, 2016), a finite element software for advanced structural analysis. The following assumptions are adopted for

the numerical models: homogeneous masonry material in all elements of the structure, having the following mechanical properties for granite masonry (Oliveira et al., 2012): material density equal to $2,000 \text{ kg/m}^3$, Young's modulus and Poisson's ratio equal to 1 GPa and 0.2, respectively. The vertical walls have the same thickness in each model and, for simplicity, the external wall openings (windows, small doors, etc.) are not considered in the numerical models. Finally, a rigid ground foundation (all elements are fixed at the base) is assumed. **Figures 3C,D** illustrates the implemented numerical models of

TABLE 1 | Range of parameters for the model of single nave and three naves.

		HNV (m)	HNVmin (m)	Thickness (m)	WNV (m)	WMC (m)	LNV (m)	LMAX (m)	WBT (m)*	HBT (m)*
Single nave	Min	7.20	–	0.50	6.00	4.50	13.20	20.10	2.45	12.20
	Max	25.00	–	2.30	16.00	11.00	41.00	57.00	5.15	42.50
Three naves	Min	6.50	3.90	0.50	12.00	4.10	22.80	28.2	2.60	9.10
	Max	22.60	15.40	2.06	24.00	14.30	47.30	63.70	9.82	31.64

*Only for class T and-VT models.

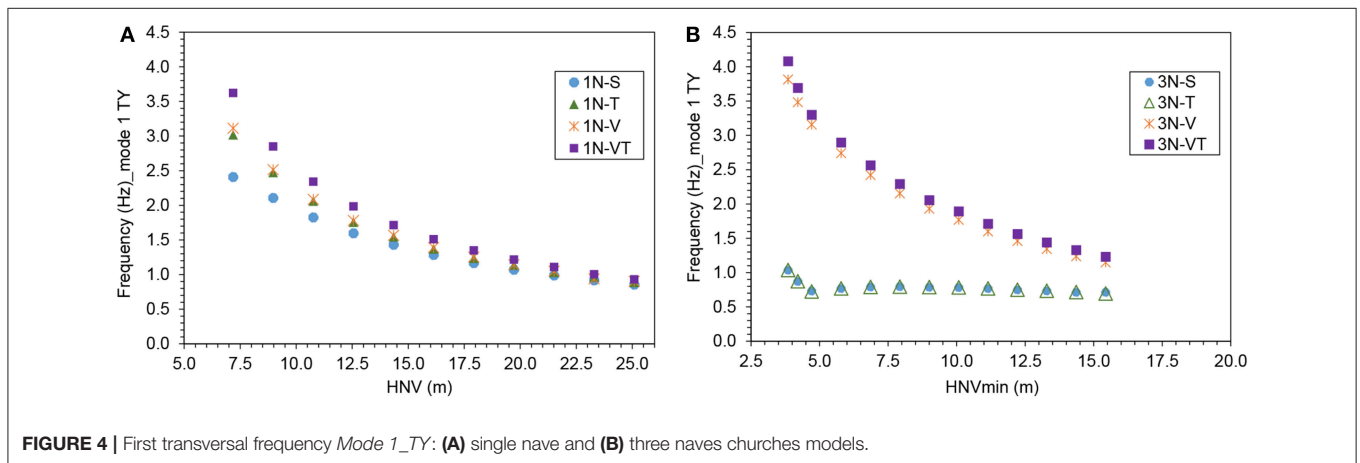


FIGURE 4 | First transversal frequency *Mode 1_TY*: (A) single nave and (B) three naves churches models.

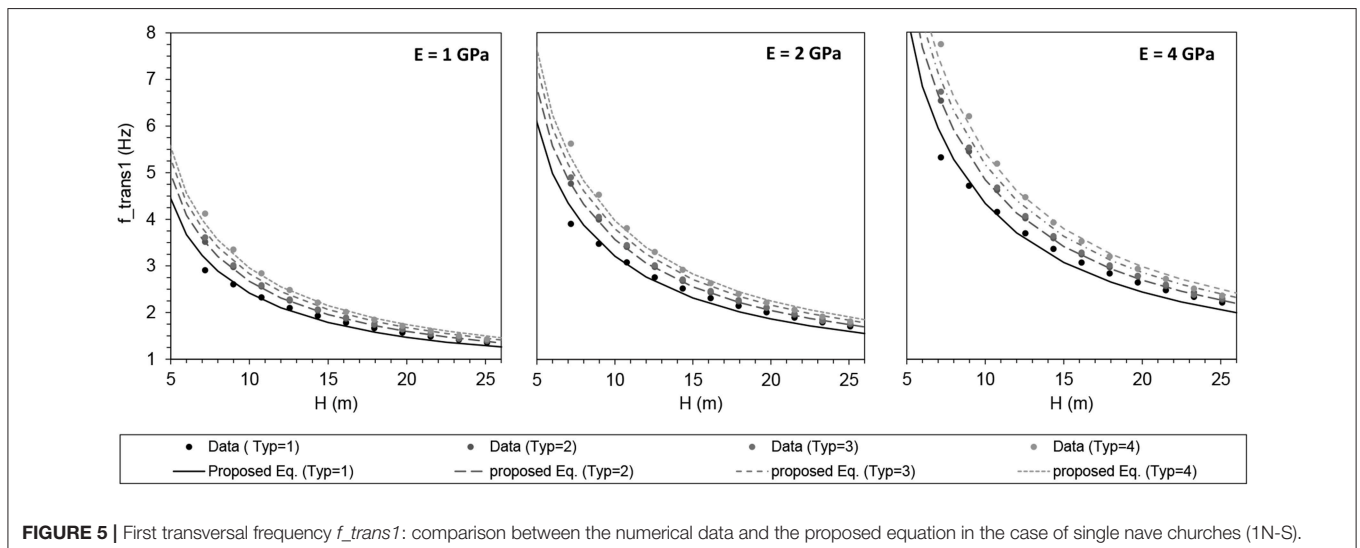


FIGURE 5 | First transversal frequency f_{trans1} : comparison between the numerical data and the proposed equation in the case of single nave churches (1N-S).

the eight church reference typologies. The assigned geometric dimensions for performing the analyses are in accordance with the proposed Equation (4, 5), by varying them into the ranges summarized in **Table 1**. It must be noted that the minimum height (*HNV*) considered for single and three naves models (7.2 and 6.5 m, respectively) corresponds to the lowest values found within the 50 Portuguese churches in the sample.

The parametric analyses are conducted using a code implemented in *MatLab R2013* (MATLAB Statistics Toolbox Release, 2013), together with *iDiana 10.1* to define the different models and to compute the natural frequencies through modal analysis. Eight-node quadrilateral isoparametric curved shell elements have been used for modeling the walls of churches and of the bell tower, six-node triangular isoparametric curved shell element for the vaults, and three-dimensional beams with three-node elements for columns. Eleven and thirteen base models are implemented in order

to perform, in total, 44 and 52 numerical models for single and three naves typology, respectively. In particular, the analyses consider the variation at the same time up to nine geometrical parameters in the case of more complex-base models. Furthermore, 55 additional models are implemented to study the influence of the Young's modulus on the response of churches type 1N-S, too.

Finally, by performing modal analyses, the main modes of vibration and frequencies of the numerical models are identified and compared. In particular, it has been observed for all the implemented models that the first vibration mode (indicated as *mode 1_TY*) is related to a global translation with simple curvature in the structure transversal direction. While, the second mode (*mode 2_TY*) corresponds to a global translation of the structure having a double curvature in the transversal direction. Finally, the third mode (*mode_TX*) represents a global translation with simple curvature in the longitudinal direction of the structure, with an overturning mechanism of the main façade. **Figure 4** shows the first transverse natural frequency *mode 1_TY* obtained for single (1N) and three (3N) naves models. It clearly illustrates that, in the case of single nave (1N models), the typologies with towers (T), vaults or both (V or VT), have always the first frequency higher than the simple model (1N-S). The comparisons confirm that the models with towers and vaults (1N-VT) are stiffer than the other ones, because the vaults significantly decrease the lateral flexibility. Moreover, it is observed that the higher the nave height, the lower the scatter among the results. In the case of three naves models (3N models) the *mode 1_TY* frequencies of models with towers (3N-T), vaults (3N-V), and both (3N-VT) do not vary significantly among them, but the result are remarkably different with respect to the simple model (3N-S).

From the obtained frequencies with the numerical analyses it is possible to propose formulas correlating the found frequencies with the main geometrical parameters of the investigated church typologies. These formulas, developed by multivariable regression analysis and separately derived for churches having a single or three naves, allow estimating the first three frequencies, that are two transversal and one longitudinal. An analytical exponential form for the proposed equations is adopted in the Equation (4), reproducing the form proposed by several international codes for calculating the fundamental period of a structure:

$$f(H, Typ, E) = a(H)^b (Typ)^c (E)^{0.5} (\text{Hz}) \quad (6)$$

where *a*, *b* and *c* are numerical coefficients; *H* is the nave height in meters (equal to *HNV* or *HNVmin* depending on the church typology); *Typ* is a coefficient related to the church type (that is S, T, V, and VT), ranging from 1 to 4, as follows: 1 for churches without towers or vaults (*S typology*), 2 for churches with only towers (*T typology*), 3 for churches having only vaults (*V typology*), and 4 in the case of churches with towers and vaults (*VT typology*); *E* is the average Young's modulus of the masonry (in GPa). With the form of the Equation (6), three relationships are proposed to estimate the three main frequencies of the two considered church types (Equations 7, 8). They refer to the first

TABLE 2 | Database of ancient masonry churches compiled from a literature review.

Numbers	Name	Location	References
1	Reggio Emilia Cathedral	Reggio Emilia (Italy)	Casarin and Modena, 2007
2	Basilica S. Maria	Collemaggio (Italy)	Antonacci et al., 2001
3	San Giovanni Battista	Matera (Italy)	Ulloque, 2017
4	Matera Cathedral	Matera (Italy)	Ramirez et al., 2019
5	Church of Monastery of Jerónimos	Lisbon (Portugal)	Ramos et al., 2010
6	Church of Monastery of Jesus	Setúbal (Portugal)	Araújo and Lourenço, 2011
7	N. Sra. do Carmo	Lagos (Portugal)	Mendes et al., 2005
8	Our Lady of Conception	Portalegre (Portugal)	Mendes et al., 2016a
9	Saint Torcato	Guimaraes (Portugal)	Ramos et al., 2013
10	Saint Miguel de Refojos	Refojos de Basto (Portugal)	Ramirez, 2016
11	Church of Ínsua de São Isidro	Caminha (Portugal)	Granda et al., 2019
12	Mallorca Cathedral	Majorca (Spain)	Elyamani et al., 2017
13	St. Nicholas Cathedral	Famagusta (Cyprus)	Votsis et al., 2012
14	St. Mamas	Morphou (Cyprus)	Votsis et al., 2012
15	Nossa Senhora das Dores	Ceará (Brazil)	Mesquita et al., 2017
16	Metropolitan Cathedral of Santiago	Santiago (Chile)	Torres et al., 2017
17	San Juan Bautista of Huaro	Cusco (Peru)	Aguilar et al., 2016
18	Kuño Tambo Church	Cusco (Peru)	Mendes et al., 2016b
19	Ica Cathedral	Ica (Peru)	Lourenço et al., 2016

two transversal global mode shapes (indicated as *Transversal 1* and *Transversal 2*) and to the first longitudinal global mode shape (*Longitudinal 1*). For the proposed equation the resulting correlation coefficient R^2 is reported, too. As it is possible to note, for all the proposed formulas a very good correlation with the numerical results is obtained. For sake of completeness, **Figure 5** compares the first frequencies f_{trans1} numerically derived with the proposed equations, in the case of single nave simple model (*1N-S*) and when varying the Young's modulus E .

• *Single Nave*

$$\begin{cases} \text{Transversal 1 : } f_{trans1} = 18.509 \cdot \text{HNV}^{-0.985} \cdot \text{Typ}^{0.178} \cdot E^{0.5} \quad (R^2 = 0.99) \\ \text{Transversal 2 : } f_{trans2} = 34.234 \cdot \text{HNV}^{-0.929} \cdot \text{Typ}^{-0.203} \cdot E^{0.5} \quad (R^2 = 0.91) \\ \text{Longitudinal 1 : } f_{long1} = 18.509 \cdot \text{HNV}^{-0.985} \cdot \text{Typ}^{0.178} \cdot E^{0.5} \quad (R^2 = 0.85) \end{cases} \quad (7)$$

• *Three Naves*

$$\begin{cases} \text{Transversal 1 : } f_{trans1} = 2.437 \cdot \text{HNV}^{-0.743} \cdot \text{Typ}^{1.101} \cdot E^{0.5} \quad (R^2 = 0.94) \\ \text{Transversal 2 : } f_{trans2} = 11.468 \cdot \text{HNV}^{-0.821} \cdot \text{Typ}^{-0.368} \cdot E^{0.5} \quad (R^2 = 0.89) \\ \text{Longitudinal 1 : } f_{long1} = 15.461 \cdot \text{HNV}^{-0.836} \cdot \text{Typ}^{0.197} \cdot E^{0.5} \quad (R^2 = 0.87) \end{cases} \quad (8)$$

COMPARISON WITH EXPERIMENTAL RESULTS

Once simplified formulations for estimating the modal frequencies of some typologies of churches has been proposed, a database of case studies is collected in order to compare the experimental results with the ones obtained with the proposed relationships. In this scope, a set of 19 ancient masonry churches is defined through a literature review in order to define a database

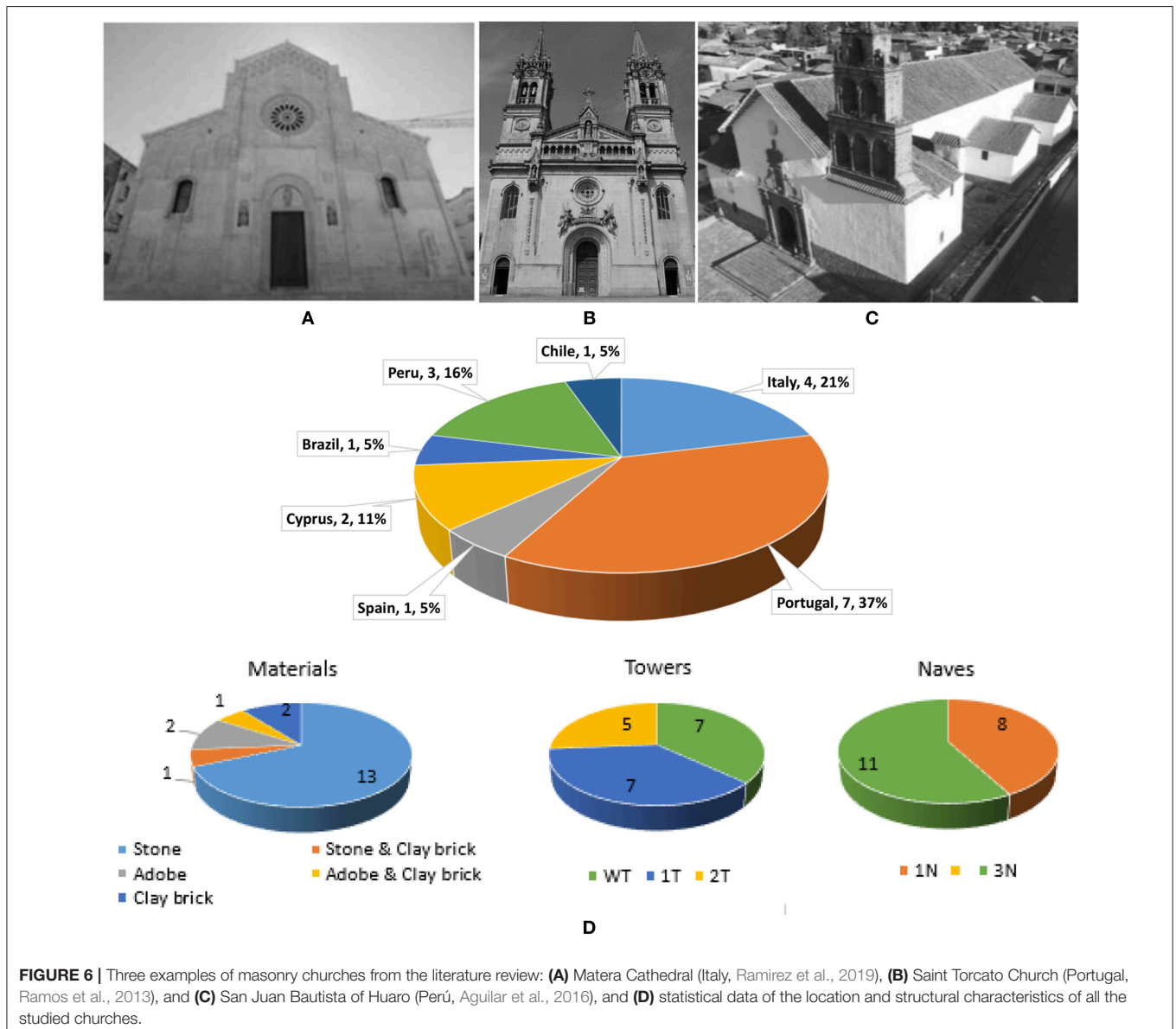


FIGURE 6 | Three examples of masonry churches from the literature review: **(A)** Matera Cathedral (Italy, Ramirez et al., 2019), **(B)** Saint Torcato Church (Portugal, Ramos et al., 2013), and **(C)** San Juan Bautista de Huaró (Perú, Aguilar et al., 2016), and **(D)** statistical data of the location and structural characteristics of all the studied churches.

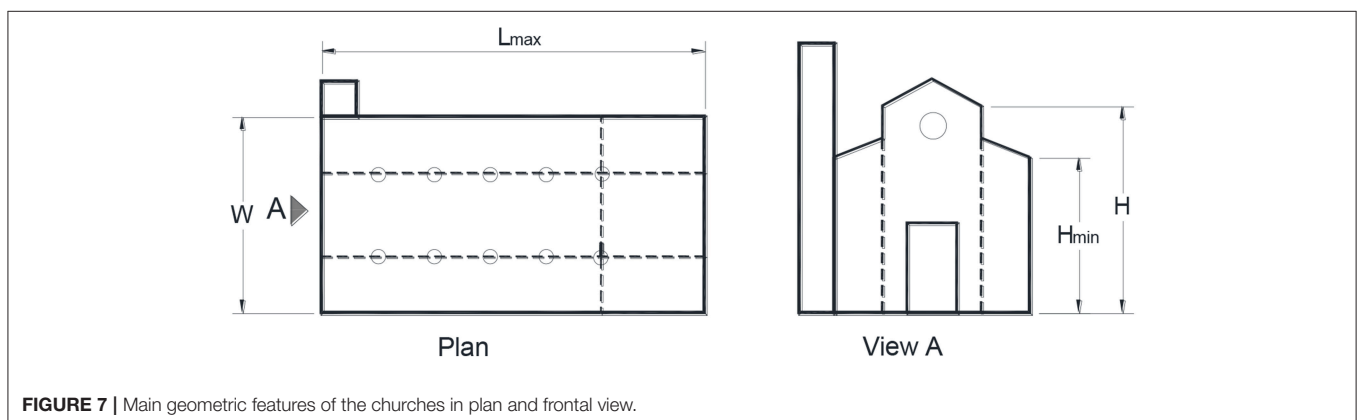
of experimental tests results. The experimental tests have been performed with the aim of determining the dynamic properties and material characteristics of churches, for detecting damages and also for assessing their seismic performances. **Table 2** reports the list of the chosen case studies with the related location and literature reference. For completeness, **Figure 6** reports three of the selected masonry churches located, respectively, in Italy, Portugal, and Peru, as representative of the considered churches. **Figure 6A** shows the Matera Cathedral in Southern Italy built in the thirteenth century, which is an example of the Apulian Romanesque architecture. It is constituted by three naves, having a Latin cross plan covered with a timber roof, and also a tall bell tower. The church was built with stone masonry, using the local calcarenite rock (Ramirez et al., 2019). **Figure 6B** illustrates the main façade of the Saint Torcato church in Guimarães (Northern Portugal), an example of the so-called Neo-Manueline style built at the end of the nineteenth century. The church structure is

composed by different materials, such as granite stone in most of the elements and concrete in the apse. It presents the typical Latin cross plan with a single nave covered by a barrel vault, and a transept having a dome in the center. In the past, the church presented significant structural problems, such as cracks in the main and lateral façade and leaning towers due the settlement of the foundation. Recently, the church has been equipped with a monitoring system to evaluate the strengthening interventions applied (Ramos et al., 2013). Lastly, **Figure 6C** depicts the San Juan Bautista of Huaró located in Cusco (Southern Peru). The church belongs to the Andean baroque style and its construction dates back to the sixteenth century. It consists of adobe masonry walls for the main structural system, having a single nave with a bell tower. The foundations are in stone masonry and the roofing system is made using timber collar trusses (Aguilar et al., 2016).

Figure 6D illustrates the geographical distribution of the 19 chosen churches, all built between the ninth and the nineteenth

TABLE 3 | Main geometrical characteristics and collected frequencies from the published literature.

Numbers	Name	H (m)	Hmin (m)	Lmax (m)	W (m)	fexp_trans1 (Hz)	fexp_trans2 (Hz)	fexp_long1 (Hz)
1	Reggio Emilia Cathedral	20.7	15.3	77.0	33.0	2.65	3.33	3.02
2	Basilica S. Maria	18.3	12.3	10.5	31.0	1.25	1.72	–
3	San Giovanni Battista	12.0	6.0	18.7	14.0	5.45	7.47	5.90
4	Matera Cathedral	15.8	9.1	56.3	20.5	2.22	4.54	3.42
5	Church of Monastery of Jerónimos	22.7	20.5	70.0	40.0	3.70	–	6.30
6	Church of Monastery of Jesus	12.5	10.5	41.6	12.2	3.53	4.22	–
7	N. Sra. do Carmo	9.0	–	35.4	7.2	3.30	–	–
8	Our Lady of Conception	7.0	–	21.1	6.3	6.23	10.09	10.46
9	Saint Torcato	19.3	–	57.5	17.5	2.14	2.93	2.63
10	Saint Miguel de Refojos	15.5	–	64.0	24.0	2.75	3.72	4.07
11	Church of Ínsua de São Isidro	4.0	–	18.1	6.4	6.00	9.84	–
12	Mallorca Cathedral	43.9	29.4	120.0	55.0	1.58	1.94	1.43
13	St. Nicholas Cathedral	21.0	16.0	50.0	25.0	1.04	1.40	0.98
14	St. Mamas	8.0	7.5	18.0	8.0	1.95	2.47	–
15	Nossa Senhora das Dores	10.0	–	26.2	11.9	2.39	2.88	3.13
16	Metropolitan Cathedral of Santiago	17.0	15.0	110.0	30.0	1.90	2.19	–
17	San Juan Bautista of Huaró	10.0	–	50.0	11.6	2.16	2.56	3.60
18	Kuño Tambo Church	6.0	–	34.0	11.0	1.59	2.68	2.15
19	Ica Cathedral	6.5	6.5	52.4	21.0	2.84	3.22	3.94



centuries having comparable construction technology and types of materials. It can be observed that the majority of the studied churches are located in Portugal (37%) and Italy (21%), but there are also churches located in Peru, Cyprus, Chile, Spain and Brazil. **Figure 6D** depicts as well the chosen churches grouped in terms of construction materials (such as stone, adobe, clay brick, stone, or adobe with clay brick), configuration and number of naves. It is worth to note that the most common material is stone, that was a material largely used in the monumental construction. As far as the structural configuration is concerned, the chosen churches are almost equally divided in those without tower (*type WT*), having a single (*type 1T*) or two towers (2T). In terms of naves, within the chosen group it is possible to find eight churches having a single nave and 13 with three naves.

Table 3 provides, for each examined church, the identified geometrical parameters and the resulting main frequencies obtained by the means of dynamic identification tests. In detail, it is reported the main nave height (*H*), the lateral naves height (*Hmin*), the maximum length (*Lmax*), and width (*W*) in plan, as illustrated in **Figure 7**. As far as the obtained experimental results are concerned, **Table 3** lists all the found frequencies collected in literature, namely *fexp_trans1* and *fexp_trans2* corresponding to first and second main frequency in the transversal direction, and *fexp_long1*, which is the first frequency in the longitudinal direction.

The found frequencies have been experimentally measured through dynamic identification tests carried out acquiring, depending on the case, ambient vibrations or artificial excitation (instrumented hammer or vibrodyne). All the churches have been instrumented with accelerometers, whose locations have been defined starting from preliminary modal analyses obtained with FE models. Uniaxial or triaxial accelerometers sensors have been used recording signals in a variable interval from 10 to 30 min in the case of ambient vibrations tests, with a sample rate of 100–200 SPS (Samples per second). The accelerometers have been placed on the churches elements considered more representative from a dynamic point of view (e.g., façade, nave, etc.).

Comparative Assessment

This section compares the collected experimental frequencies, summarized in the **Table 3** with the ones empirically estimated with the formulas of (ASCE 07-16, 2017) (Equation 1), (NTC-2008, 2008) (Equation 2), (NCSE-2002, 2002) (Equation 3). Moreover, also the new proposed equations are considered. In particular, **Figures 8A,B** compare the frequencies predicted with the code equations with the ones corresponding to the first experimental transverse frequency *fexp_trans1*. As it is possible to observe, the scatter among data is not negligible and only in few cases the considered code formulations approximate the experimental frequencies. Most likely, this is due to the fact that the frequencies of the churches do not only depend on the structures height, but also on the other geometrical characteristics and mechanical properties. As for the (NCSE-2002, 2002) formulation, it leads to considerable frequency overestimations because of, while the experimental values are ranging from 1 to 6 Hz, the predicted ones result from 5 to 30 Hz. The remarkable gap among the experimental and predicted frequencies is probably due to the fact that the (NCSE-2002, 2002) formula has been calibrated starting from masonry structures stiffer than the churches. Moreover, the comparison experimental values *fexp_trans1* against the

TABLE 4 | RMSE and *R*² coefficients obtained comparing the experimental *fexp_trans1*, *fexp_trans2*, and *fexp_long1* with the predicted values (Equations 7, 8).

Frequency		RMSE	<i>R</i> ²
First transverse <i>fexp_trans1</i>	(NTC-2008, 2008; ASCE 07-16, 2017)	1.52	0.26
	(NCSE-2002, 2002)	10.64	0.03
	Proposed formulation	1.26	0.52
Second transverse <i>fexp_trans2</i>	(NCSE-2002, 2002)	37.0	0.03
	Proposed formulation	1.7	0.58
First Longitudinal <i>fexp_long1</i>	(NCSE-2002, 2002)	63.7	0.001
	Proposed formulation	1.9	0.45

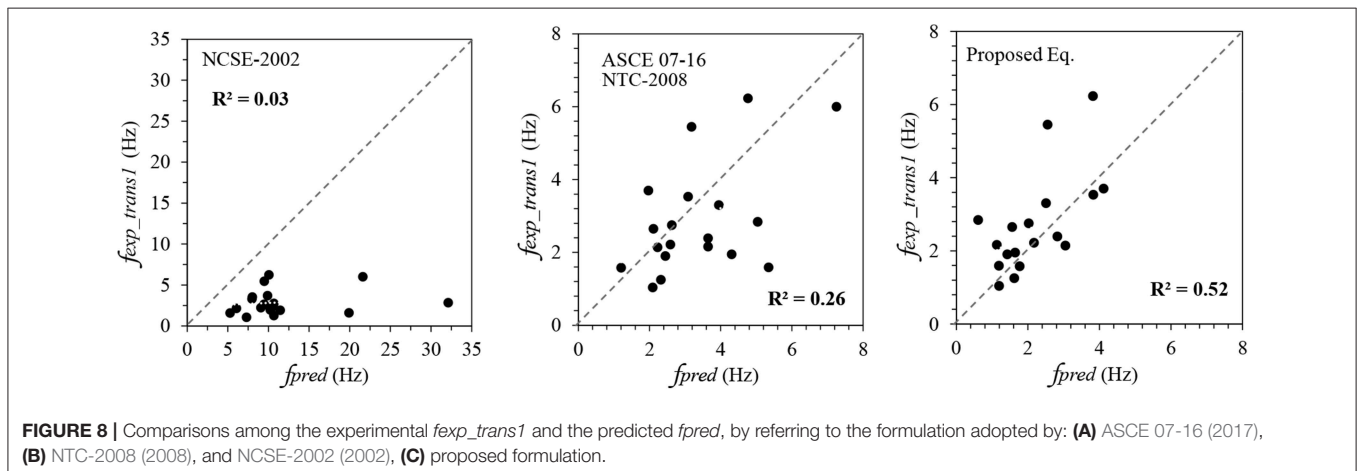


FIGURE 8 | Comparisons among the experimental *fexp_trans1* and the predicted *fpred*, by referring to the formulation adopted by: **(A)** ASCE 07-16 (2017), **(B)** NTC-2008 (2008), and **(C)** proposed formulation.

predicted ones with proposed equations (Equations 7, 8) in **Figure 8C** is reported.

For all the comparisons considered, the resulting errors among the predicted and experimental values are measured in this study through two statistics parameters, that are *Root Mean Squared Error* (RMSE) and *R-squared* (R^2), calculated as follows:

1. The RMSE parameter, representing the square root of the variance of the residuals, given by the expression [Equation (5)]:

$$RMSE = \sqrt{\frac{\sum_{i=1}^n (f_{exp,i} - f_{1,i})^2}{n}} \quad (9)$$

where $f_{exp,i}$ and $f_{1,i}$ are the experimental and predicted frequencies, and n is the number of data points. The lower the RMSE parameter the higher the accuracy in prediction of the experimental frequencies.

2. The R^2 factor, calculated as follows:

$$R^2 = 1 - \frac{\sum_{i=1}^n (f_{exp,i} - f_{1,i})^2}{\sum_{j=1}^n (f_{exp,j} - \frac{\sum_{i=1}^n f_{exp,i}}{n})^2} \quad (10)$$

Where with the same symbols of the previous Equation (9). Therefore, the higher values of R^2 indicate that the regression model fits the data better.

The numerical values of the RMSE and R^2 obtained in the analyzed cases are reported in **Table 4**. As far as the first transverse frequency f_{exp_trans1} is concerned, it is clear that all the considered formulations, with exception for the proposed one, have a scarce accuracy in predicting the experimental values due, most likely, to the fact that these formulations, as already remarked, have been proposed for generic masonry buildings and not specifically for churches. Moreover, although the (NCSE-2002, 2002) formulation should result more accurate because it considers two parameters, this code standard provides the worst prediction. In contrast, the proposed formulation fits better the experimental data ($R^2 = 0.52$ and $RMSE = 1.26$). For sake of completeness, **Table 4** also reports the resulting errors RMSE and R^2 among the predicted and experimental values in the case of the second transverse (f_{exp_trans2}) and first longitudinal (f_{exp_long1}) frequency. In these cases, the errors are calculated by referring only to the analytical formulations where it has been possible to calculate the predicted values, that are the (NCSE-2002, 2002) formulation and the proposed one. As it is possible to note, an acceptable accuracy with the proposed formulation (Equations 7, 8) is also obtained in these cases.

Formulations Based on Experimental Data

In addition to the proposed equations (Equations 7, 8) derived from numerical simulations with finite element models, in this paragraph simplified formulations for the first transverse frequency are also proposed, directly derived from the set of the considered experimental results. In particular, three different types of equations are proposed having an exponential form including, respectively, one, two and three variables. They are derived with regression

TABLE 5 | Results of the regression analysis for estimate the first frequency using one-variable, two-variable and three-variable formulas.

ONE-VARIABLE FORMULAS						
Numbers	Formula	a	b	R^2		
1	aH^b	9.25	-0.477	0.26		
2	$aH^{-0.75}$	16.53	-	0.18		
3	aW^b	11.29	-0.505	0.31		
4	$a(L_{max})^b$	7.07	-0.246	0.11		
TWO-VARIABLE FORMULAS						
Numbers	Formula	a	b	c	R^2	
1	$aH^b(L_{max})^c$	13.06	-0.411	-0.152	0.28	
2	aH^bW^c	12.21	-0.171	-0.380	0.32	
3	aH^bE^c	13.84	-0.669	-0.249	0.55	
4	$aH^bE^{0.5}$	15.76	-0.815	-	0.33	
5	$aW^b(L_{max})^c$	14.33	-0.446	-0.111	0.32	
6	aW^bE^c	14.81	-0.634	0.233	0.51	
7	$a(L_{max})^bE^c$	6.69	-0.237	0.077	0.14	
THREE-VARIABLE FORMULAS						
Numbers	Formula	a	b	c	d	R^2
1	$aH^bW^cE^d$	15.99	-0.425	-0.274	0.247	0.57
2	$aH^bW^cE^{0.5}$	19.73	-0.414	-0.446	0.5	0.39

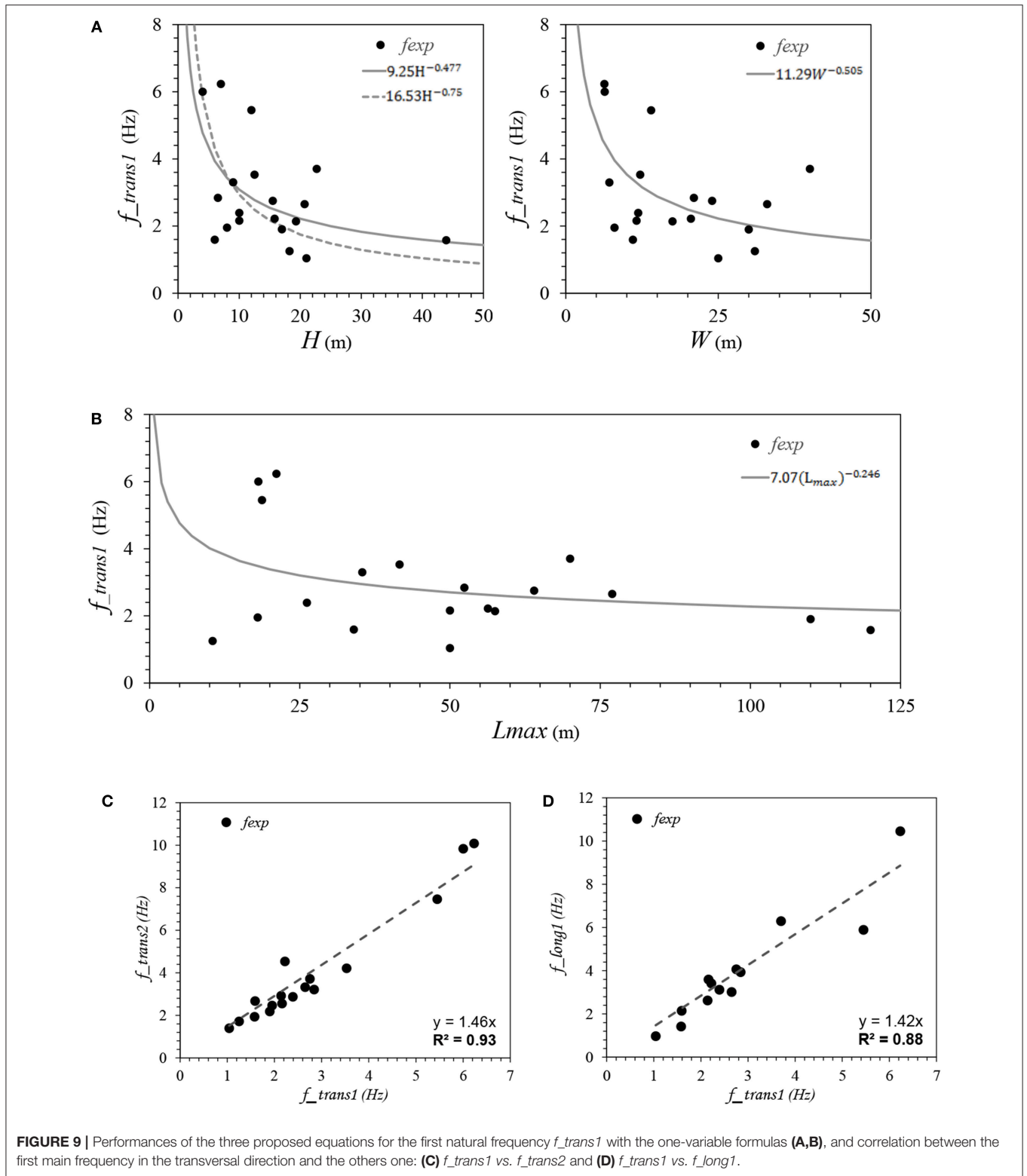
analysis by using the software *CurveExpert Professional* (Hyams, 2011).

The simplest proposed formula has the following exponential form:

$$f_{trans1} = aV^b \quad (\text{Hz}) \quad (11)$$

That is the usual formulation adopted by design codes, where V represents a geometrical parameter (given in meters) such as, for instance, H (height of the main nave), or W (width in plan) or L_{max} (maximum length in plan), as shown in the **Figure 7**; a and b are regression coefficients, for a confidence level equal to 95%.

Table 5 reports the proposed formulas having a single variable form of the Equation (11) with the resulting R^2 factor. The same formulas are graphically reported in **Figures 9A,B**, and compared with the collected experimental values. Each of the proposed formulation considers separately the most important factors influencing the first transverse frequency of a church, that is the height (H) for the *Formula 1* and *Formula 2*, the transverse dimension in plan (W) for the *Formula 3*, and the length in plan (L_{max}) for the *Formula 4*. In particular, the *Formula 2* is similar to the *Formula 1*, where the variable H is also chosen as principal geometrical parameter for defining the dynamic behavior of a church. In this last formula its exponent b is assumed equal to -0.75 in order to maintain the same analytical structure of the fundamental period equation proposed by the considered national codes (Equations 1, 2). Finally, by comparing the different one-variable formulations proposed, it is easy to note that, in terms of scatter (**Table 5**), the lower errors are obtained in the cases of *Formula 1* and the *Formula 3* confirming that, for predicting the first natural frequency of a structure the significant parameters are the height H and transverse dimension W along which the oscillation occurs.



As for the two-variable models (Table 5), the considered parameters are, again, H , W , L_{max} and the further Young's modulus E . It is easy to note that the proposed formulations considering the parameter length in plan

L_{max} (such as the formulas 1, 5, and 7) provide the lowest matching with the experimental data. On the other hand, the models including the parameter E , either considering the height H (Formula 3) or W (Formula 6)

TABLE 6 | List of the sampled churches data illustrated in **Figure 2**.

ID	Church	Location	District	Architectural style (main)
1	Armamar Cathedral	Armamar	Viseu	Romanesque
2	Basílica da Estrela	Lapa	Lisboa	Neoclassical
3	Bravães	Bravães	Viana do Castelo	Romanesque
4	Bustêlo Monastery	Penafiel	Porto	Baroque
5	Cabeça Santa	Penafiel	Porto	Romanesque
6	Caminha Cathedral	Caminha	Viana do Castelo	Gothic
7	Clérigos	Porto	Porto	Baroque
8	Golegã Cathedral	Golegã	Santarém	Manueline
9	Grijó Monastery	Vila Nova de Gaia	Porto	Manueline
10	Lapa	Porto	Porto	Neoclassical
11	Leça do Bailio Monastery	Leça do Bailio	Porto	Gothic
12	Santa Casa de Misericórdia	Évora	Évora	Baroque
13	Pombeiro (Mosteiro)	Pombeiro de Ribavizela	Porto	Romanesque
14	Salvador	Paço de Sousa	Porto	Gothic
15	Santa Clara	Porto	Porto	Gothic
16	Santa Clara	Vila do Conde	Porto	Gothic
17	Santa Maria da Azurara	Vila do Conde	Porto	Manueline
18	Santo Ildelfonso	Porto	Porto	Baroque
19	S. Bento de Cástris Convent	Évora	Évora	Manueline
20	São Francisco	Évora	Évora	Manueline
21	São Frutuoso	Braga	Braga	Visigothic
22	São Gens de Boelhe/Igreja Velha	Penafiel	Porto	Romanesque
23	Moura Cathedral	Moura	Beja	Manueline
24	Igreja de São João da Foz	Porto	Porto	Baroque
25	São Lourenço de Almancil	Loulé	Faro	Baroque
26	São Lourenço—Grilos Convent	Porto	Porto	Manueline
27	São Lourenço—V. N. Azeitão	Sesimbra	Setúbal	Baroque
28	São Martinho de Cedofeita	Cedofeita	Porto	Romanesque
29	São Miguel de Nevogilde	Porto	Porto	Baroque
30	São Pedro de Cête	Paredes	Porto	Romanesque
31	São Pedro de Ferreira	Paços de Ferreira	Porto	Romanesque
32	São Pedro da Lourosa	Oliveira do Conde	Coimbra	Visigothic
33	São Pedro de Rates	Póvoa de Varzim	Porto	Romanesque
34	São Pedro de Roriz	Roriz	Porto	Romanesque
35	Braga Cathedral	Braga	Braga	Baroque
36	Lamego Cathedral	Lamego	Viseu	Romanesque
37	Porto Cathedral	Porto	Porto	Romanesque
38	Silves Cathedral	Silves	Faro	Gothic
39	Tibães Monastery	Tibães	Braga	Baroque
40	Viana do Alentejo Cathedral	Viana do Alentejo	Évora	Manueline
41	Vila do Bispo Cathedral	Vila do Bispo	Faro	Baroque
42	Vila do Conde Cathedral	Vila do Conde	Porto	Manueline
43	Vouzela Cathedral	Vouzela	Viseu	Romanesque
44	Nossa Senhora da Conceição	Alto Alentejo	Portalegre	Manueline
45	São Torcato	Guimaraes	Braga	Manueline
46	Santa Maria de Gondar	Gondar	Porto	Romanesque
47	Capela nostra senhora da insua	Caminha	Viana do Castelo	Romanesque
48	Arronches Cathedral	Arronches	Portalegre	Manueline
49	Redinha Cathedral	Pombal	Leira	Manueline
50	Santo Amaro	Beja	Beja	Gothic

provide the best correlation (R^2 equal to 0.55 and 0.51, respectively).

For completeness, also three-variable models are suggested starting from the regression analyses on the experimental data collected (Table 5). For these formulas the chosen variables are the height and the width in plan (H and W), and the material Young's Modulus (E). Among the formulations proposed, Formula 1 allows us to obtain a better match with the experimental results ($R^2 = 0.57$), also with respect to the Formula 1 with having two variables. The Formula 2, although is similar to the Formula 1, differs for the fact that the third coefficient d is fixed to 0.50, for establishing a formula similar to the proposed in Table 4. Finally, as it is clear to see, the best model to predict the first main frequency in the transversal direction is with three-variables is the following formula having the minor error and a value of $R^2 = 0.56$:

$$f_{trans1} = 16.41H^{-0.4}W^{-0.3}E^{0.2} \quad (12)$$

Determination of the Two Subsequent Natural Frequencies

Starting from the collected experimental data of Table 5, a preliminary formula also for correlating the two subsequent natural frequencies (f_{trans2} and f_{long1}) with the first one is presented (f_{trans1}). The correlations found between the second (f_{trans2}) and the first longitudinal (f_{long1}) frequencies with the first one (f_{trans1}) are reported in Equations (13, 14).

$$f_{trans2} = 1.46 (f_{trans1}) \quad (13)$$

$$f_{long1} = 1.42 (f_{trans1}) \quad (14)$$

The same correlations are plotted in the Figures 9C,D and compared with the experimental values. As it is clear to observe, in the cases analyzed the relationships of f_{trans2} and f_{long1} with f_{trans1} may be both described with an acceptable error with linear formulations.

CONCLUSIONS

In this paper, simplified formulas for estimating the main frequencies of ancient masonry churches have been proposed. They represent also a practical tool for revealing potential hidden damages or the actual connections among the parts since the estimated values may be compared with the ones obtained through dynamic identification tests. The proposed formulations have been derived with multivariable regressions starting from the numerical results of analyses carried out with finite elements models. In these analyses the geometric parameters have been varied in accordance with specific relationships derived by studying the proportioning of 50 existing ancient churches. In particular, the numerical simulations addressed ancient churches having one or three naves with/without bell towers and vaults.

The proposed equations derived from numerical simulations, unlike the ones indicated in seismic design codes, have the characteristic of being particularly appropriate for the ancient churches typology, and not for general masonry buildings. Moreover, specific equations for estimating the second transverse

frequency and the first longitudinal have been also derived. The comparisons with a set of experimental data collected in the published literature validate the simplified formulations, demonstrating that a better estimation of the frequency may be done by accounting, in the numerical proposed formulations, of simultaneously the nave height, the type of structure and the Young's modulus. It should be remarked that the considered design code formulations (NCSE-2002, 2002; NTC-2008, 2008; ASCE 07-16, 2017) tend to overestimate the main frequency of a structure and have a weak correlation with the actual values. On the contrary, as demonstrated the proposed formulations have a good accuracy in predicting the experimental frequencies.

Finally, preliminary numerical formulas are also proposed directly established with numerical regressions on the considered experimental data. These formulas have one-, two- or three-variables and conserve an exponential form, in analogy with the classic form adopted by seismic design codes. The best accuracy in predicting the experimental data is reached with a three-variables formulation considering the two dimensions in plan and a representative Young's modulus.

In future the proposed equations may be improved by considering also the actual damage of the elements/parts, as well as of considering interventions, existing or to be applied. In addition, it should be possible also to explicitly take into account the presence and efficiency of additional elements (such as buttress among the others) that, as known, significantly influence the transversal frequency of a structure. Finally, it should be remarked that the investigations performed in this paper are based on the key assumption that all the typologies considered exhibit a whole structural behavior. Therefore, before their application, one should carefully exclude partial responses of some element, by duly investigating through *in-situ* tests all the structural details.

ANNEX: LIST OF THE SAMPLED CHURCHES DATA

Table 6 reports the list of the sampled churches data.

AUTHOR CONTRIBUTIONS

All authors listed have made a substantial, direct and intellectual contribution to the work, and approved it for publication.

ACKNOWLEDGMENTS

The research activity carried out by SL has been supported by the ELARCH scholarship and mobility, a project funded under the Erasmus Mundus Action 2 Partnership (EMA2) by the European Commission, and coordinated by the University of Basilicata (www.elarch.org). ELARCH project: Reference number 552129-EM-1-2014-1-IT-ERA MUNDUS-EMA21 funded with support of the European Commission. This document reflects the view only of the author, and the Commission cannot be held responsible for any use which may be made of the information contained therein.

REFERENCES

- Aguilar, R., Noel, M., Briceño, C., Arce, D., and Castañeda, B. (2016). "Geomatics" procedures and dynamic identification for the structural survey of the church of "San Juan Bautista de Huaro" in Peru," in *16th International Brick and Block Masonry Conference*, eds C. Modena, F. da Porto, and M. R. Valluzzi (Padova: CRC Press), 815–820.
- Antonacci, E., Beolchini, G. C., Di Fabio, F., and Gattulli, V. (2001). "The dynamic behavior of the Basilica S. Maria of Collemaggio," in *2nd International Congress on Studies in Ancient Structures* (Istanbul).
- Araújo, A. S., and Lourenço, P. B. (2011). "Avaliação Da Segurança Sísmica De Igrejas: Aplicação a Dois Casos De Estudo," in *Congresso de Métodos Numéricos em Engenharia 2011* (Coimbra: APMTAC).
- ASCE 07-16 (2017). *Minimum Design Loads and Associated Criteria for Buildings and Other Structures* American Society of Civil Engineers. Virginia, NV: Reston.
- Bartoli, G., Betti, M., Marra, A. M., and Monchetti, S. (2017). Semiempirical formulations for estimating the main frequency of slender masonry towers. *J. Perform. Constr. Facilit.* 31, 1–10. doi: 10.1061/(ASCE)CF.1943-5509.0001017
- Caprili, S., Mangini, F., Salvatore, W., Bevilacqua, M. G., Karwacka Codini, E., Squeglia, N., et al. (2017). A knowledge-based approach for the structural assessment of cultural heritage, a case study: La Sapienza Palace in Pisa. *Bull. Earthq. Eng.* 15, 4851–4886. doi: 10.1007/s10518-017-0158-y
- Casarin, F., and Modena, C. (2007). "Dynamic identification of S. Maria Assunta Cathedral, Reggio Emilia, Italy," in *2nd International Operational Modal Analysis Conference* (Copenhagen), 637–644.
- D'Amato, M., Laterza, M., and Casamassima, V. M. (2017). Seismic performance evaluation of a multi-span existing masonry arch bridge. *Open Constr. Build. Technol. J.* 11(Suppl. 5), 1191–1207. doi: 10.2174/1874149501711011191
- D'Amato, M., Laterza, M., and Diaz Fuentes, D. (2018). Simplified seismic analyses of ancient churches in matera's landscape. *Int. J. Archit. Heritage*. doi: 10.1080/15583058.2018.1511000. [Epub ahead of print].
- De Luca, F., Verderame, G. M., and Manfredi, G. (2014). Eurocode-based seismic assessment of modern heritage RC structures: The case of the Tower of the Nations in Naples (Italy). *Eng. Struct.* 74, 96–110. doi: 10.1016/j.engstruct.2014.05.015
- Diaferio, M., Foti, D., and Potenza, F. (2018). Prediction of the fundamental frequencies and modal shapes of historic masonry towers by empirical equations based on experimental data. *Eng. Struct.* 156, 433–442. doi: 10.1016/j.engstruct.2017.11.061
- Douglas, B., and Reid, W. (1982). Dynamic test and system identification of bridges. *J. Struct. Div.* 108, 2295–2312.
- Ellis, B. R., and BRE. (1998). Non-destructive dynamic testing of stone pinnacles on the Palace of Westminster. *Proc. Instit. Civil Eng. Struct. Build.* 128, 300–307.
- Elyamani, A., Caselles, O., Roca, P., and Clapes, J. (2017). Dynamic investigation of a large historical cathedral. *Struct. Control Health Monitor.* 24:e1885. doi: 10.1002/stc.1885
- Formisano, A., and Marzo, A. (2017). Simplified and refined methods for seismic vulnerability assessment and retrofitting of an Italian cultural heritage masonry building. *Comput. Struct.* 180, 13–26. doi: 10.1016/j.compstruc.2016.07.005
- Formisano, A., Vaiano, G., Fabbrocino, F., and Milani, G. (2018). Seismic vulnerability of Italian masonry churches: The case of the Nativity of Blessed Virgin Mary in Stellata of Bondeno. *J. Build. Eng.* 20, 179–200. doi: 10.1016/j.job.2018
- Fuentes, D. D., Laterza, M., and D'Amato, M. (2019). "Seismic vulnerability and risk assessment of historic constructions: the case of masonry and adobe churches in Italy and Chile," in *Proceedings of SAHC 2018, 11th International Conference on Structural Analysis of Historical Constructions* (Cusco), 1127–1137.
- Goel, R. K., and Chopra, A. K. (1997). Period formulas for moment-resisting frame buildings. *J. Struct. Eng.* 11, 1454–1461.
- Granda, S., López, S., Navia, F., Ramirez, E., Ramirez, R., Ramos, L. F., et al. (2019). "Diagnosis and structural assessment of the fortress and convent of Ínsua de São Isidro BT," in *Proceedings of SAHC 2018, 11th International Conference on Structural Analysis of Historical Constructions* (Cusco), 2386–2394.
- Hyams, D. G. (2011). *CurveExpert Professional. V. 2.6.3*. Available online at: <https://www.curveexpert.net/>
- Krstevska, L., Tashkov, L., Naumovski, N., Florio, G., Formisano, A., Fornaro, A., et al. (2010). "In-situ experimental testing of four historical buildings damaged during the 2009 L'Aquila earthquake," in *COST ACTION C26: Urban Habitat Constructions under Catastrophic Events - Proceedings of the Final Conference* (Naples), 427–432.
- Lagamarsino, S., and Resemini, S. (2009). The assessment of damage limitation state in the seismic analysis of monumental buildings. *Earthq. Spectra* 25, 323–346. doi: 10.1193/1.3110242
- Laterza, M., D'Amato, M., and Casamassima, V. M. (2017). "Seismic performance evaluation of multi-span existing masonry arch bridge," in *Proceedings of the 14th International Conference of Numerical Analysis and Applied Mathematics - ICNAAM 2016* (Rhodes).
- Lourenço, P. B., Karanikoloudis, G., and Greco, F. (2016). "In situ testing and modeling of cultural heritage buildings in Peru, proceedings of SAHC 2016," in *10th International Conference on Structural Analysis of Historical Constructions* (Leuven), 850–857.
- Lourenço, P. B., Oliveira, D. V., Leite, J. C., Ingham, J. M., Modena, C., and da Porto, F. (2013). Simplified indexes for the seismic assessment of masonry buildings: international database and validation. *Eng. Fail. Anal.* 34, 585–605. doi: 10.1016/j.engfailanal.2013.02.014
- Luchin, G., Ramos, L. F., and D'Amato, M. (2018). Sonic tomography for masonry walls characterization. *Int. J. Architect. Heritage*. doi: 10.1080/15583058.2018.1554723. [Epub ahead of print].
- MATLAB and Statistics Toolbox Release (2013). *The MathWorks, Inc.*, Natick, MA.
- Mendes, N., Lourenço, P. B., Besca, M., Truffelli, E., and Barontini, A. (2016a). Diagnosis and seismic analysis of the Our Lady of Conception Church, Portugal. Case studies of building pathology in cultural heritage. *Build. Pathol. Rehab.* 1, 1–21. doi: 10.1007/978-981-10-0639-5_10
- Mendes, N., Zanotti, S., Lourenço, P. B., and Lemos, J. (2016b). "Análise sísmica da Igreja de Kuño Tambo," in *10º Congresso Nacional de Sismologia e Engenharia Sísmica* (Ponta Delgada).
- Mendes, P., Baptista, M. A., Agostinho, L., Lagomarsino, S., and Costa, J. P. (2005). "Structural and dynamic analysis of N. Sra. do Carmo church, Lagos Portugal," in *Proceedings EURO-DYN2005* (Paris), 311–318.
- Mesquita, E., Brandão, F., Diogenes, A., Antunes, P., and Varum, H. (2017). Ambient vibrational characterization of the Nossa Senhora das Dores Church. *Eng. Struct. Technol.* 9, 170–182. doi: 10.3846/2029882X.2017.1416311
- NCSE-2002 (2002). *Norma de Construcción Sismorresistente. Parte General y Edificación* (Spanish Standard)- Ministerio de Fomento.
- NTC-2008 (2008). *Norme Tecniche per le Costruzioni. D.M. 14/01/2008, S.O. n. 30 of the Official Gazette of the Italian Republic 2008.*
- NTC-2018 (2018). *Aggiornamento delle Norme Tecniche per le Costruzioni. D.M. 17/01/2018, S.O. n. 42 of the Official Gazette of the Italian Republic 2018.*
- Oliveira, D. V., Silva, R. A., Garbin, E., and Lourenço, P. B. (2012). Strengthening of three-leaf stone masonry walls: an experimental research. *Mater. Struct.* 45, 1259–1276. doi: 10.1617/s11527-012-9832-3
- Ramirez, E., Lourenço, P. B., and D'Amato, M. (2019). "Seismic assessment of the Matera Cathedral," in *Proceedings of SAHC 2018, 11th International Conference on Structural Analysis of Historical Constructions* (Cusco) 1346–1354.
- Ramirez, R. (2016). *Structural Analysis of the Church of the Monastery of São Miguel de Refojos*. Guimarães: University of Minho.
- Ramos, L. F., Aguilar, R., Lourenço, P. B., and Moreira, S. (2013). Dynamic structural health monitoring of Saint Torcato church. *Mech. Syst. Signal Process.* 35, 1–15. doi: 10.1016/j.ymsp.2012.09.007
- Ramos, L. F., Marques, L., Lourenço, P. B., De Roeck, G., Campos-Costa, A., and Roque, J. (2010). Monitoring historical masonry structures with operational modal analysis: Two case studies. *Mech. Syst. Signal Process.* 24, 1291–1305. doi: 10.1016/j.ymsp.2010.01.011
- Ranieri, C., and Fabbrocino, G. (2011). "Predictive correlations for the estimation of the elastic period of masonry towers masonry towers," in *4th International Conference on Experimental Vibration Analysis for Civil Engineering Structures* (Varenna). Available online at: <https://www.researchgate.net>
- Ranieri, C., Fabbrocino, G., and Verderame, G. M. (2013). Non-destructive characterization and dynamic identification of a modern heritage building for serviceability seismic analyses. *NDT E Int.* 60, 17–31. doi: 10.1016/j.ndteint.2013.06.003

- Sarhosis, V., Milani, G., Formisano, A., and Fabbrocino, F. (2018). Evaluation of different approaches for the estimation of the seismic vulnerability of masonry towers. *Bull. Earthq. Eng.* 16, 1511–1545. doi: 10.1007/s10518-017-0258-8
- Shakya, M., Varum, H., Vicente, R., and Costa, A. (2016). Empirical formulation for estimating the fundamental frequency of slender masonry structures. *Int. J. Architect. Heritage* 10, 55–66. doi: 10.1080/15583058.2014.951796
- TNO (2016). *Displacement method ANALyser- DIANA FEA BV- iDiana Release 10.1*.
- Torres, W., Almazán, J. L., Sandoval, C., and Boroschek, R. (2017). Operational modal analysis and FE model updating of the Metropolitan Cathedral of Santiago, Chile. *Eng. Struct.* 143, 168–188. doi: 10.1016/j.engstruct.2017.04.008
- Ulloque, E. (2017). *Seismic Assessment of the Church San Giovanni Battista*. Matera: University of Minho.
- Votsis, R. A., Kyriakides, N., Chrysostomou, C. Z., Tantele, E., and Demetriou, T. (2012). Ambient vibration testing of two masonry monuments in Cyprus. *Soil Dyn. Earthq. Eng.* 43, 58–68. doi: 10.1016/j.soildyn.2012.07.015

Conflict of Interest Statement: The authors declare that the research was conducted in the absence of any commercial or financial relationships that could be construed as a potential conflict of interest.

Copyright © 2019 Lopez, D'Amato, Ramos, Laterza and Lourenço. This is an open-access article distributed under the terms of the Creative Commons Attribution License (CC BY). The use, distribution or reproduction in other forums is permitted, provided the original author(s) and the copyright owner(s) are credited and that the original publication in this journal is cited, in accordance with accepted academic practice. No use, distribution or reproduction is permitted which does not comply with these terms.